Formation of superheavy nuclei in cold fusion reactions

Zhao-Qing Feng,[1,2] Gen-Ming Jin,[1] Jun-Qing Li,[1] and Werner Scheid[3]
[1]*Institute of Modern Physics, Chinese Academy of Sciences, Lanzhou 730000, People's Republic of China*
[2]*Gesellschaft für Schwerionenforschung mbH (GSI), D-64291 Darmstadt, Germany*
[3]*Institut für Theoretische Physik der Universität, D-35392 Giessen, Germany*
(Received 19 July 2007; published 16 October 2007)

Within the concept of the dinuclear system (DNS), a dynamical model is proposed for describing the formation of superheavy nuclei in complete fusion reactions by incorporating the coupling of the relative motion to the nucleon transfer process. The capture of two heavy colliding nuclei, the formation of the compound nucleus, and the de-excitation process are calculated by using an empirical coupled channel model, solving a master equation numerically and applying statistical theory, respectively. Evaporation residue excitation functions in cold fusion reactions are investigated systematically and compared with available experimental data. Maximal production cross sections of superheavy nuclei in cold fusion reactions with stable neutron-rich projectiles are obtained. Isotopic trends in the production of the superheavy elements $Z = 110$, 112, 114, 116, 118, and 120 are analyzed systematically. Optimal combinations and the corresponding excitation energies are proposed.

DOI: 10.1103/PhysRevC.76.044606 PACS number(s): 25.70.Jj, 24.10.−i, 25.60.Pj, 24.60.−k

I. INTRODUCTION

The synthesis of very heavy (superheavy) nuclei is a very important subject in nuclear physics, motivated with respect to the theoretically predicted island of stability, and has obtained much experimental progress with fusion-evaporation reactions [1,2]. The existence of superheavy nuclei (SHN) ($Z \geqslant 106$) is due to a strong binding shell effect against the large Coulomb repulsion. However, the shell effect gets reduced with increasing excitation energy of the formed compound nucleus. Combinations with a doubly magic nucleus or nearly magic nucleus are usually chosen owing to the larger reaction Q values. Reactions with ^{208}Pb or ^{209}Bi targets were first proposed by Oganessian *et al*. to synthesize SHN [3]. Six new elements with $Z = 107$–112 were synthesized in cold fusion reactions for the first time and investigated at GSI (Darmstadt, Germany) with the heavy-ion accelerator UNILAC and the separator SHIP [1,4]. Recently, experiments on the synthesis of element 113 in the ^{70}Zn + ^{209}Bi reaction have been performed successfully at RIKEN (Tokyo, Japan) [5]. Superheavy elements $Z = 113$–116, 118 were synthesized at FLNR in Dubna (Russia) with double magic nucleus ^{48}Ca bombarding actinide nuclei [6]. Reasonable understanding on the formation of SHN in massive fusion reactions is still a challenge for theory.

In accordance with the evolution of two heavy colliding nuclei, the whole process of the compound nucleus formation and decay is usually divided into three reaction stages, namely the capture process of the colliding system to overcome Coulomb barrier, the formation of the compound nucleus to pass over the inner fusion barrier, and the de-excitation of the excited compound nucleus against fission. The transmission in the capture process depends on the incident energy and relative angular momentum of the colliding nuclei and is the same as in the fusion of light- and medium-mass systems. The complete fusion of the heavy system after capture in competition with quasifission is very important in the estimation of the SHN production. At present it is still difficult to make an accurate description of the fusion dynamics. After the capture and the subsequent evolution to form the compound nucleus, the thermal compound nucleus will decay by the emission of light particles and γ rays against fission. These three stages will affect the formation of evaporation residues observed in laboratories. The evolution of the whole process of massive heavy-ion collisions is very complicated at near-barrier energies. Most of theoretical approaches to the formation of SHN have a similar viewpoint in the description of the capture and the de-excitation stages, but there is no consensus on the compound nucleus formation process. There are mainly two sorts of models, depending on whether the compound nucleus is formed along the radial variable (internuclear distance) or by nucleon transfer at the minimum position of the interaction potential after capture of the colliding system. Several transport models have been established to understand the fusion mechanism of two heavy colliding nuclei leading to SHN formation, such as the macroscopic dynamical model [7,8], the fluctuation-dissipation model [9], the concept of nucleon collectivization [10], and the dinuclear system model [11]. With these models experimental data can be reproduced and some new results have been predicted. The models differ from each other, and sometimes contradictory physical ideas are used.

Further improvements of these models have to be made. Here we use an improved dinuclear system (DNS) model, in which the nucleon transfer is coupled with the relative motion and the barrier distribution of the colliding system is included. We present a new and extended investigation of the production of superheavy nuclei in lead-based cold fusion reactions. For that we make use of a formalism describing the nucleon transfer with a set of microscopically derived master equations.

In Sec. II we give a description on the DNS model. Calculated results of fusion dynamics and SHN production in cold fusion reactions are given in Sec. III. In Sec. IV conclusions are discussed.

II. DINUCLEAR SYSTEM MODEL

The dinuclear system is a molecular configuration of two touching nuclei that keep their own individuality [11]. Such a system has an evolution along two main degrees of freedom: (i) the relative motion of the nuclei in the interaction potential to form the DNS and the decay of the DNS (quasifission process) along the R degree of freedom (internuclear motion) and (ii) the transfer of nucleons in the mass asymmetry coordinate $\eta = (A_1 - A_2)/(A_1 + A_2)$ between two nuclei, which is a diffusion process of the excited systems leading to the compound nucleus formation. Off-diagonal diffusion in the surface (A_1, R) is not considered because we assume the DNS is formed at the minimum position of the interaction potential of two colliding nuclei. In this concept, the evaporation residue cross section is expressed as a sum over partial waves with angular momentum J at the center-of-mass energy $E_{\mathrm{c.m.}}$,

$$\sigma_{\mathrm{ER}}(E_{\mathrm{c.m.}}) = \frac{\pi\hbar^2}{2\,\mu E_{\mathrm{c.m.}}} \sum_{J=0}^{J_{\max}} (2J+1) T(E_{\mathrm{c.m.}}, J) \times P_{\mathrm{CN}}(E_{\mathrm{c.m.}}, J) W_{\mathrm{sur}}(E_{\mathrm{c.m.}}, J). \quad (1)$$

Here, $T(E_{\mathrm{c.m.}}, J)$ is the transmission probability of the two colliding nuclei overcoming the Coulomb potential barrier in the entrance channel to form the DNS. In the same manner as in the nucleon collectivization model [10], the transmission probability T is calculated by using the empirical coupled channel model, which can reproduce very well available experimental capture cross sections [10,12]. P_{CN} is the probability that the system will evolve from a touching configuration into the compound nucleus in competition with quasifission of the DNS and fission of the heavy fragment. The last term is the survival probability of the formed compound nucleus, which can be estimated with the statistical evaporation model by considering the competition between neutron evaporation and fission [12]. We take the maximal angular momentum as $J_{\max} = 30$ since the fission barrier of the heavy nucleus disappears at high spin [13].

To describe the fusion dynamics as a diffusion process in mass asymmetry, we have used the analytical solution of the Fokker-Planck equation [11] and the numerical solution of the master equation [14,15], which were also used to treat deep inelastic heavy-ion collisions. Here, the fusion probability is obtained by solving a master equation numerically in the potential energy surface of the DNS. The time evolution of the distribution function $P(A_1, E_1, t)$ for fragment 1 with mass number A_1 and excitation energy E_1 is described by the following master equation [16,17]:

$$\frac{dP(A_1, E_1, t)}{dt} = \sum_{A_1'} W_{A_1, A_1'}(t)\big[d_{A_1} P(A_1', E_1', t) - d_{A_1'} P(A_1, E_1, t)\big] - [\Lambda^{\mathrm{qf}}(\Theta(t)) + \Lambda^{\mathrm{fis}}(\Theta(t))] P(A_1, E_1, t). \quad (2)$$

Here $W_{A_1, A_1'}$ is the mean transition probability from the channel (A_1, E_1) to (A_1', E_1'), and d_{A_1} denotes the microscopic dimension corresponding to the macroscopic state (A_1, E_1). The sum is taken over all possible mass numbers that fragment A_1' may take (from 0 to $A = A_1 + A_2$), but only one nucleon transfer is considered in the model with $A_1' = A_1 \pm 1$. The excitation energy E_1 is the local excitation energy ε_1^* with respect to fragment A_1, which is determined by the dissipation energy from the relative motion and the potential energy of the corresponding DNS and will be shown later in Eqs. (8) and (9). The dissipation energy is described by the parametrization method of the classical deflection function [18,19]. The motion of nucleons in the interacting potential is governed by the single-particle Hamiltonian [12,14]

$$H(t) = H_0(t) + V(t), \quad (3)$$

with

$$H_0(t) = \sum_K \sum_{\nu_K} \varepsilon_{\nu_K}(t) a_{\nu_K}^\dagger(t) a_{\nu_K}(t),$$
$$V(t) = \sum_{K,K'} \sum_{\alpha_K, \beta_{K'}} u_{\alpha_K, \beta_{K'}}(t) a_{\alpha_K}^\dagger(t) a_{\beta_{K'}}(t) = \sum_{K,K'} V_{K,K'}(t). \quad (4)$$

Here the indices $K, K'(K, K' = 1, 2)$ denote the fragments 1 and 2. The quantities ε_{ν_K} and $u_{\alpha_K, \beta_{K'}}$ represent the single-particle energies and the interaction matrix elements, respectively. The single-particle states are defined with respect to the centers of the interacting nuclei and are assumed to be orthogonalized in the overlap region. So the annihilation and creation operators depend on time. The single-particle matrix elements are parameterized by

$$u_{\alpha_K, \beta_{K'}}(t) = U_{K,K'}(t) \left\{ \exp\left[-\frac{1}{2} \left(\frac{\varepsilon_{\alpha_K}(t) - \varepsilon_{\beta_{K'}}(t)}{\Delta_{K,K'}(t)} \right)^2 \right] - \delta_{\alpha_K, \beta_{K'}} \right\}, \quad (5)$$

which contains some parameters $U_{K,K'}(t)$ and $\Delta_{K,K'}(t)$. The detailed calculation of these parameters and the mean transition probabilities were described in Refs. [12,14].

The evolution of the DNS along the variable R leads to the quasifission of the DNS. The quasifission rate Λ^{qf} can be estimated with the one-dimensional Kramers formula [20,21]

$$\Lambda^{\mathrm{qf}}(\Theta(t)) = \frac{\omega}{2\pi\omega^{B_{\mathrm{qf}}}} \left(\sqrt{\left(\frac{\Gamma}{2\hbar} \right)^2 + (\omega^{B_{\mathrm{qf}}})^2} - \frac{\Gamma}{2\hbar} \right) \times \exp\left(-\frac{B_{\mathrm{qf}}(A_1, A_2)}{\Theta(t)} \right). \quad (6)$$

Here the quasifission barrier measures the depth of the pocket of the interaction potential. The local temperature is given by the Fermi-gas expression $\Theta = \sqrt{\varepsilon^\star/a}$ corresponding to the local excitation energy $\varepsilon^\star$ and level density parameter $a = A/12\ \mathrm{MeV}^{-1}$. In Eq. (6) $\omega^{B_{\mathrm{qf}}}$ is the frequency of the inverted harmonic oscillator approximating the interaction potential of two nuclei in R around the top of the quasifission barrier, and ω is the frequency of the harmonic oscillator approximating the potential in R at the bottom of the pocket. The quantity Γ denotes the double average width of the contributing single-particle states, which determines the friction coefficients: $\gamma_{ii'} = \frac{\Gamma}{\hbar}\,\mu_{ii'}$, with $\mu_{ii'}$ being the inertia

tensor. Here we use constant values $\Gamma = 2.8$ MeV, $\hbar\omega^{B_{\rm qf}} = 2.0$ MeV, and $\hbar\omega = 3.0$ MeV for the following reactions. The Kramers formula is derived at the quasistationary condition of the temperature $\Theta(t) < B_{\rm qf}(A_1, A_2)$. However, the numerical calculation in Ref. [21] indicated that Eq. (6) is also available at the condition of $\Theta(t) > B_{\rm qf}(A_1, A_2)$. In the reactions of synthesizing SHN, there is the possibility of the fission of the heavy fragment in the DNS. Because the fissility increases with the charge number of the nucleus, the fission of the heavy fragment can affect the quasifission and fusion when the DNS evolves toward larger mass asymmetry. The fission rate $\Lambda^{\rm fis}$ can also be treated with the one-dimensional Kramers formula [20]

$$\Lambda^{\rm fis}(\Theta(t)) = \frac{\omega_{\rm g.s.}}{2\pi\omega_f}\left(\sqrt{\left(\frac{\Gamma_0}{2\hbar}\right)^2 + \omega_f^2} - \frac{\Gamma_0}{2\hbar}\right) \times \exp\left(-\frac{B_f(A_1, A_2)}{\Theta(t)}\right), \tag{7}$$

where $\omega_{\rm g.s.}$ and ω_f are the frequencies of the oscillators approximating the fission-path potential at the ground state and on the top of the fission barrier for nucleus A_1 or A_2 (larger fragment), respectively. Here, we take $\hbar\omega_{\rm g.s.} = \hbar\omega_f = 1.0$ MeV, $\Gamma_0 = 2$ MeV. The fission barrier is calculated as a sum of a macroscopic part and the shell correction used in Ref. [22]. The fission of the heavy fragment doe not favor the diffusion of the system to a light fragment distribution. Therefore, it leads to a slightly decrease of the fusion probability [see Eq. (17)].

In the relaxation process of the relative motion, the DNS will be excited by the dissipation of the relative kinetic energy. The excited system opens a valence space $\Delta\varepsilon_K$ in fragment $K(K = 1, 2)$, which has a symmetrical distribution around the Fermi surface. Only the particles in the states within the valence space are actively involved in excitation and transfer. The averages on these quantities are performed in the valence space:

$$\Delta\varepsilon_K = \sqrt{\frac{4\varepsilon_K^*}{g_K}}, \quad \varepsilon_K^* = \varepsilon^*\frac{A_K}{A}, \quad g_K = \frac{A_K}{12}, \tag{8}$$

where ε^* is the local excitation energy of the DNS, which provides the excitation energy for the mean transition probability. There are $N_K = g_K\Delta\varepsilon_K$ valence states and $m_K = N_K/2$ valence nucleons in the valence space $\Delta\varepsilon_K$, which give the dimension

$$d(m_1, m_2) = \binom{N_1}{m_1}\binom{N_2}{m_2}.$$

The local excitation energy is defined as

$$\varepsilon^* = E_x - [(U(A_1, A_2) - U(A_P, A_T)], \tag{9}$$

where $U(A_1, A_2)$ and $U(A_P, A_T)$ are the driving potentials of fragments A_1, A_2 and fragments A_P, A_T (at the entrance point of the DNS), respectively. The excitation energy E_x of the composite system is converted from the relative kinetic energy loss, which is related to the Coulomb barrier B [23] and determined for each initial relative angular momentum J by the parametrization method of the classical deflection function [18,19]. So E_x is coupled with the relative angular momentum.

The potential energy surface (PES; i.e., the driving potential) of the DNS is given by

$$U(A_1, A_2, J, \mathbf{R}; \beta_1, \beta_2, \theta_1, \theta_2) = B(A_1) + B(A_2) - \left[B(A) + V_{\rm rot}^{\rm CN}(J)\right] + V(A_1, A_2, J, \mathbf{R}; \beta_1, \beta_2, \theta_1, \theta_2) \tag{10}$$

with $A_1 + A_2 = A$. Here $B(A_i)(i = 1, 2)$ and $B(A)$ are the negative binding energies of the fragment A_i and the compound nucleus A, respectively, in which the shell and the pairing corrections are included reasonably; $V_{\rm rot}^{\rm CN}$ is the rotation energy of the compound nucleus; the β_i represent quadrupole deformations of the two fragments; the θ_i denote the angles between the collision orientations and the symmetry axes of deformed nuclei. The interaction potential between fragment $1(Z_1, A_1)$ and $2(Z_2, A_2)$ includes the nuclear, Coulomb, and centrifugal parts as

$$V(A_1, A_2, J, \mathbf{R}; \beta_1, \beta_2, \theta_1, \theta_2) = V_N(A_1, A_2, \mathbf{R}; \beta_1, \beta_2, \theta_1, \theta_2) + V_C(A_1, A_2, \mathbf{R}; \beta_1, \beta_2, \theta_1, \theta_2) + \frac{J(J+1)\hbar^2}{2\mu\mathbf{R}^2}, \tag{11}$$

where the reduced mass is given by $\mu = m \cdot A_1A_2/A$ with the nucleon mass m. The nuclear potential is calculated by using the double-folding method based on the Skyrme interaction force without considering the momentum and the spin dependence as [24]

$$V_N = C_0\left\{\frac{F_{\rm in} - F_{\rm ex}}{\rho_0}\left[\int \rho_1^2(\mathbf{r})\rho_2(\mathbf{r} - \mathbf{R})d\mathbf{r} + \int \rho_1(\mathbf{r})\rho_2^2(\mathbf{r} - \mathbf{R})d\mathbf{r}\right] + F_{\rm ex}\int \rho_1(\mathbf{r})\rho_2(\mathbf{r} - \mathbf{R})d\mathbf{r}\right\}, \tag{12}$$

with

$$F_{\rm in,ex} = f_{\rm in,ex} + f'_{\rm in,ex}\frac{N_1 - Z_1}{A_1}\frac{N_2 - Z_2}{A_2}, \tag{13}$$

which is dependent on the nuclear densities and on the orientations of deformed nuclei in the collision [25]. The parameters $C_0 = 300$ MeV fm^3, $f_{\rm in} = 0.09$, $f_{\rm ex} = -2.59$, $f'_{\rm in} = 0.42$, $f'_{\rm ex} = 0.54$, and $\rho_0 = 0.16$ fm^{-3} are used in the calculation. The Woods-Saxon density distributions are expressed for two nuclei as

$$\rho_1(\mathbf{r}) = \frac{\rho_0}{1 + \exp[(\mathbf{r} - \Re_1(\theta_1))/a_1]} \tag{14}$$

and

$$\rho_2(\mathbf{r} - \mathbf{R}) = \frac{\rho_0}{1 + \exp[(|\mathbf{r} - \mathbf{R}| - \Re_2(\theta_2))/a_2]}. \tag{15}$$

Here $\Re_i(\theta_i)$ $(i = 1, 2)$ are the surface radii of the nuclei with $\Re_i(\theta_i) = R_i[1 + \beta_i Y_{20}(\theta_i)]$, and the spheroidal radii are R_i. The parameters a_i represent the surface diffusion coefficients, which are taken as 0.55 fm in the calculation. The Coulomb potential is obtained by Wong's formula [26], which agrees well with the double-folding procedure. In the actual calculation, the distance $\mathbf{R}$ between the centers of the

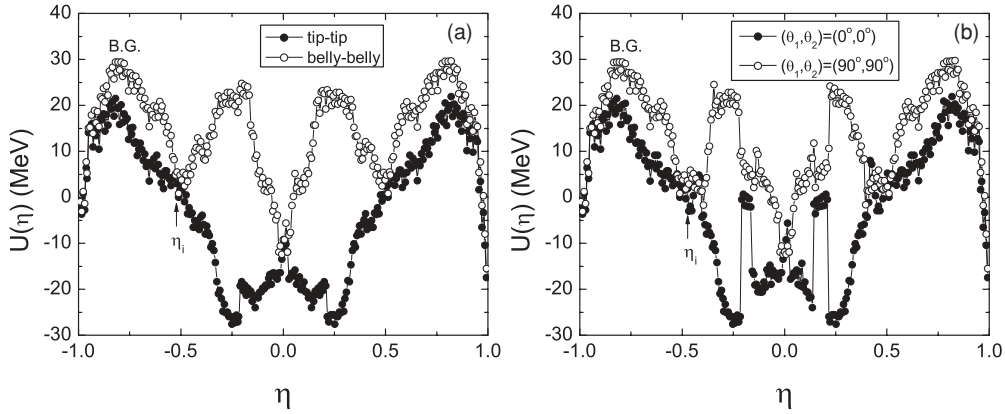

FIG. 1. The driving potential of the DNS for the reaction ^{70}Zn + ^{208}Pb as a function of the mass asymmetry η at the different orientations.

two fragments is chosen to be the value that gives the minimum of the interaction potential, in which the DNS is considered to be formed. So the PES depends only on the mass asymmetry degree of freedom η, which gives the driving potential of the DNS as shown in Fig. 1 for the reaction ^{70}Zn + ^{208}Pb at the tip-tip, the belly-belly, and the fixed $(0^\circ, 0^\circ)$ and $(90^\circ, 90^\circ)$ orientations. Here, we should note that the tip-tip orientation is different with $(0^\circ, 0^\circ)$. We rotate $\frac{\pi}{2}$ for the fragment with negative quadrupole deformation. However, the orientation angle θ_i is fixed for all fragments. The same procedure is taken for the belly-belly and $(90^\circ, 90^\circ)$. The Businaro-Gallone (B.G.) point marks the maximum position of the driving potential on the left side of the initial combination η_i. Some averaging over all orientations should be carried out in the nucleon transfer process. However, the tip-tip orientation, which gives the minimum of the PES, favors nucleon transfer and is chosen in the calculation. For the reaction ^{70}Zn + ^{208}Pb, the tip-tip orientation ($B_{\rm fus}$ = 20.98 MeV) has a lower inner fusion barrier than the belly-belly orientation ($B_{\rm fus}$ = 25.71 MeV). However, the belly-belly orientation appears to exhibit an obvious hump toward symmetric combinations (reducing $|\eta_i|$), which favors the compound nucleus formation against quasifission. Both of the two factors may affect the values of $P_{\rm CN}$ [see Eq. (17)]. In Fig. 2 we show the comparison of the formation probability of the compound nucleus in the reaction ^{70}Zn + ^{208}Pb as functions of angular momenta ($E_{\rm c.m.}$ = 254.08 MeV, $E^*_{\rm CN}$ = 12 MeV) and incident c.m. energies ($J = 0$) at the tip-tip and the belly-belly orientations, respectively. The effects of the collision orientations on the fusion cross section were also studied in detail by Nasirov *et al.* [27] for deformed combination systems.

After reaching the time of reaction in the evolution of $P(A_1, E_1, t)$, all those components on the left side of the B.G. point as shown in Fig. 1(a) contribute to the compound nucleus formation. The hindrance in the diffusion process by nucleon transfer to form the compound nucleus is the inner fusion barrier $B_{\rm fus}$, which is defined as the difference of the driving potential at the B.G. point and at the entrance position. Nucleon transfer to more symmetric fragments will favor quasifission. The formation probability of the compound nucleus at Coulomb barrier B [here the barrier distribution $f(B)$ is considered] and angular momentum J is given by

$$P_{\rm CN}(E_{\rm c.m.}, J, B) = \sum_{A_1=1}^{A_{\rm BG}} P[A_1, E_1, \tau_{\rm int}(E_{\rm c.m.}, J, B)]. \quad (16)$$

Here the interaction time $\tau_{\rm int}(E_{\rm c.m.}, J, B)$ is obtained by using the deflection function method [28]. We obtain the fusion

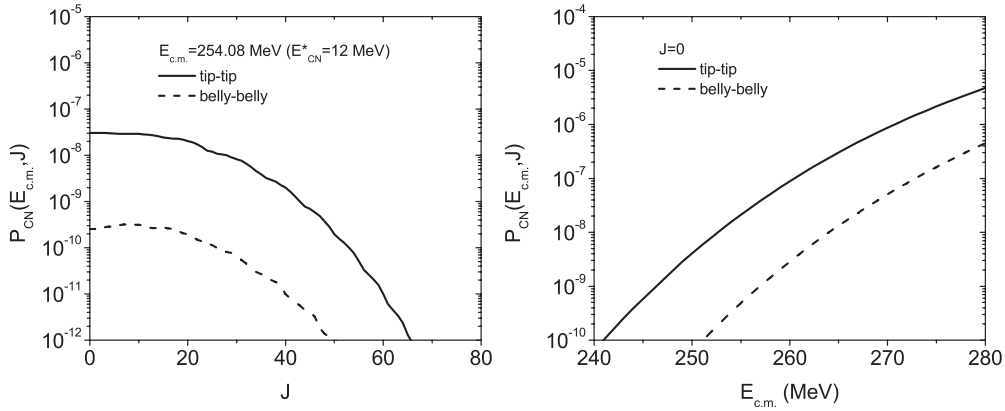

FIG. 2. Dependence of the fusion probability on angular momenta and incident c.m. energies in the reaction ^{70}Zn + ^{208}Pb at the tip-tip and the belly-belly orientations, respectively.

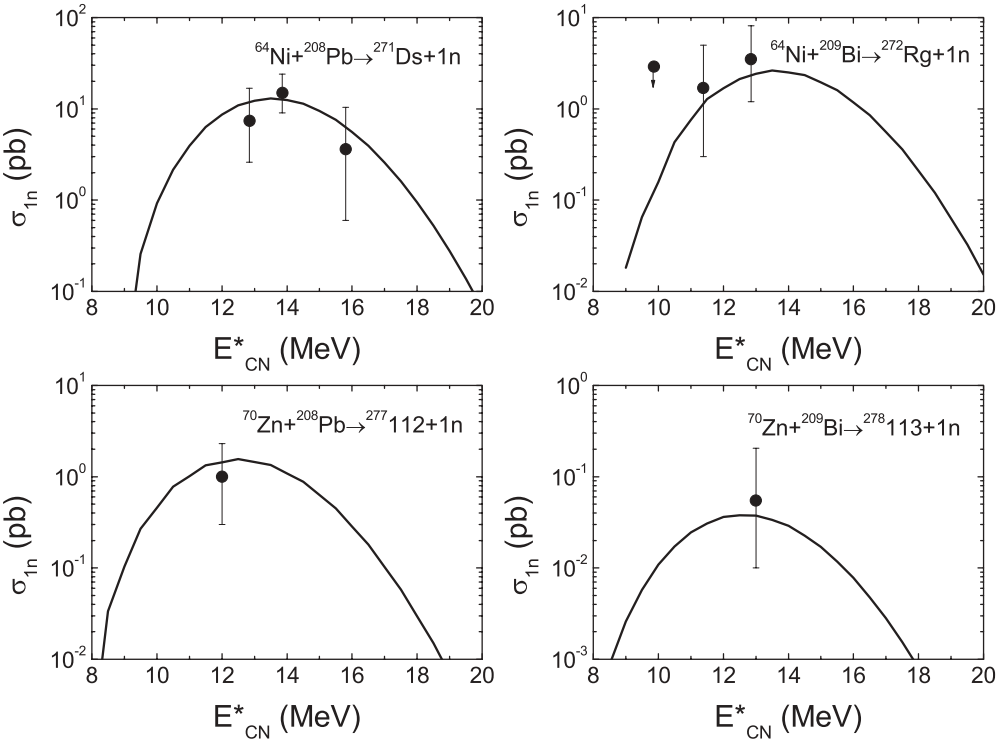

FIG. 3. Comparison of the calculated evaporation residue excitation functions and the experimental data to synthesize superheavy elements $Z = 110$–113 in cold fusion reactions.

probability as

$$P_{\mathrm{CN}}(E_{\mathrm{c.m.}}, J) = \int f(B) P_{\mathrm{CN}}(E_{\mathrm{c.m.}}, J, B) dB, \qquad (17)$$

where the barrier distribution function is taken in asymmetric Gaussian form [10,12]. So the fusion cross section is written as

$$\sigma_{\mathrm{fus}}(E_{\mathrm{c.m.}}) = \frac{\pi\hbar^2}{2\,\mu E_{\mathrm{c.m.}}} \sum_{J=0}^{\infty} (2J+1) T(E_{\mathrm{c.m.}}, J) P_{\mathrm{CN}}(E_{\mathrm{c.m.}}, J). \qquad (18)$$

The survival probability of the excited compound nucleus in the cooling process by means of the neutron evaporation in competition with fission is expressed as follows:

$$W_{\mathrm{sur}}(E^*_{\mathrm{CN}}, x, J) = P(E^*_{\mathrm{CN}}, x, J) \times \prod_{i=1}^{x} \left(\frac{\Gamma_n(E^*_i, J)}{\Gamma_n(E^*_i, J) + \Gamma_f(E^*_i, J)} \right)_i, \qquad (19)$$

where the E^*_{CN} and J are the excitation energy and the spin of the compound nucleus, respectively. E^*_i is the excitation energy before evaporating the ith neutron, which has the relation

$$E^*_{i+1} = E^*_i - B^n_i - 2T_i, \qquad (20)$$

with the initial condition $E^*_1 = E^*_{\mathrm{CN}}$. B^n_i is the separation energy of the ith neutron. The nuclear temperature T_i is given by $E^*_i = aT_i^2 - T_i$ with the level density parameter a. $P(E^*_{\mathrm{CN}}, x, J)$ is the realization probability of emitting x neutrons. The widths of neutron evaporation and fission are calculated by using the statistical model. The details can be found in Ref. [12].

III. RESULTS AND DISCUSSION

A. Evaporation residue cross sections

The evaporation residues observed in laboratories by consecutive α decay are mainly produced by the complete fusion reactions, in which the fusion dynamics and the structure properties of the compound nucleus affect their production. Within the framework of the DNS model, we calculated the evaporation residue cross sections producing SHN $Z = 110$–113 in cold fusion reactions as shown in Fig. 3, and compared them with GSI data for 110–112 [1] and RIKEN results [5] for 113. The excitation energy is obtained by $E^*_{\mathrm{CN}} = E_{\mathrm{c.m.}} + Q$, where $E_{\mathrm{c.m.}}$ is the incident energy in the center-of-mass system. The Q value is given by $Q = \Delta M_P + \Delta M_T - \Delta M_C$, and the corresponding mass defects are taken from Ref. [29] for projectile, target, and compound nucleus, respectively. Usually, neutron-rich projectiles are used to experimentally synthesize SHN, such as ^{64}Ni and ^{70}Zn, which can enhance the survival probability W_{sur} in Eq. (1) of the formed compound nucleus because of smaller neutron separation energy. The maximal production cross sections from Ds to 113 are reduced rapidly because the inner fusion barrier is increasing. Within error bars the experimental results can be reproduced very well. There are no other adjustable parameters in the calculation. Within the same scheme, we analyzed the evaporation residue excitation functions with

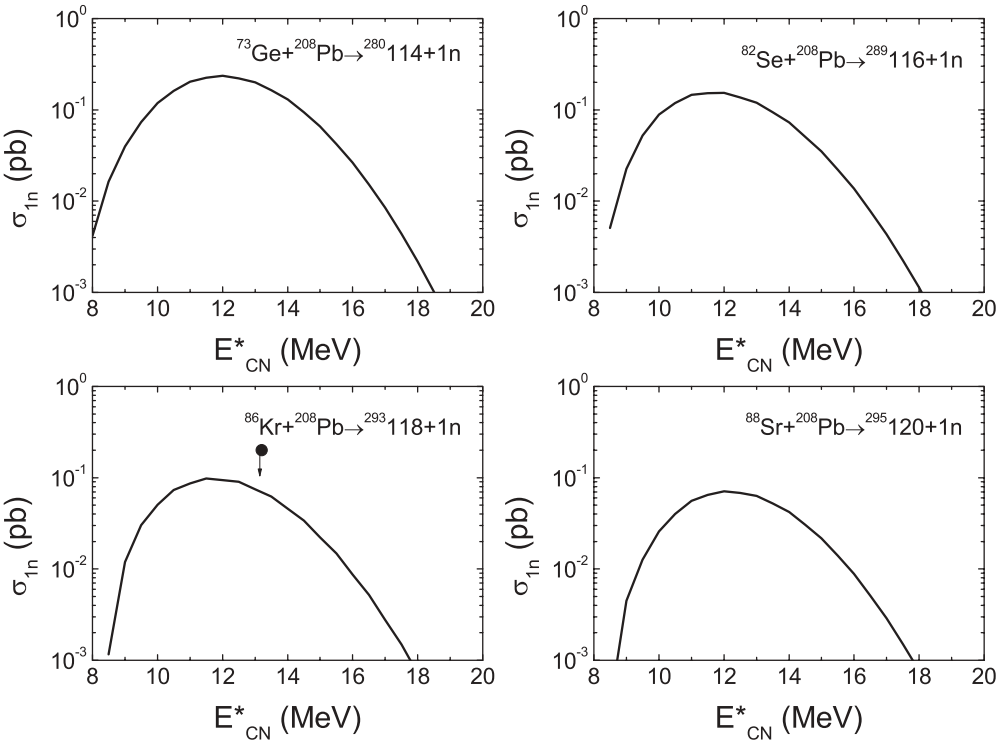

FIG. 4. The same as in Fig. 3, but for projectiles ^{73}Ge, ^{82}Se, ^{86}Kr, and ^{88}Sr in cold fusion reactions to produce superheavy elements $Z = 114$, 116, 118, and 120.

projectiles ^{73}Ge, ^{82}Se, ^{86}Kr, and ^{88}Sr to produce superheavy elements $Z = 114$, 116, 118, and 120 (Fig. 4). An upper limit for the cross section producing 118 was obtained in Berkeley [30].

In Fig. 5 we show the comparison of the calculated maximal production cross sections of superheavy elements $Z = 102$–120 in cold fusion reactions by evaporating one neutron with experimental data [1,4]. The production cross

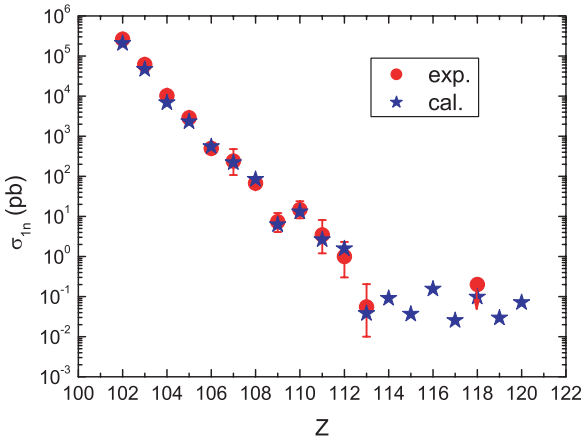

FIG. 5. (Color online) Maximal production cross sections of superheavy elements $Z = 102$–120 in cold fusion reactions based on ^{208}Pb and ^{209}Bi targets with projectile nuclei ^{48}Ca, ^{50}Ti, ^{54}Cr, ^{58}Fe, ^{64}Ni, ^{70}Zn, ^{76}Ge, ^{82}Se, ^{86}Kr, and ^{88}Sr and compared with experimental data.

sections decrease rapidly with increasing charge number of the synthesized compound nucleus, such as from 0.2 μb for the reaction ^{48}Ca + ^{208}Pb to 1 pb for ^{70}Zn + ^{208}Pb, and even below 0.1 pb for synthesizing $Z \geqslant 113$. It seems to be difficult to synthesize superheavy elements $Z \geqslant 113$ in cold fusion reactions at the present facilities. The calculated results are in good agreement with the experimental data. In the DNS concept, the inner fusion barrier increases with reducing mass asymmetry, which leads to a decrease of the formation probability of the compound nucleus, as shown in Fig. 6. However, the quasifission and the fission of the heavy fragments in the nuclear transfer process become more and more important if the mass asymmetry ($|\eta_i|$) of the projectile-target combination is decreasing, which also reduces the formation probability. There appears to be a slight increase for $Z \geqslant 118$, which is related to the decreased inner fusion barriers of the three systems. The survival of the thermal compound nucleus in the fusion reactions is mainly affected by the neutron evaporation energy, the fission barrier, and the level density. The survival probability has strong structure effects, as shown in Fig. 6. Accurate calculation of the survival probability is very necessary to obtain reasonable evaporation residue cross sections.

B. Isotopic dependence of the production cross sections

The production of SHN depends on the isotopic combination of the target and projectile in cold fusion reactions. For example, the maximal cross section is $3.5\pm^{2.7}_{1.8}$ pb for the

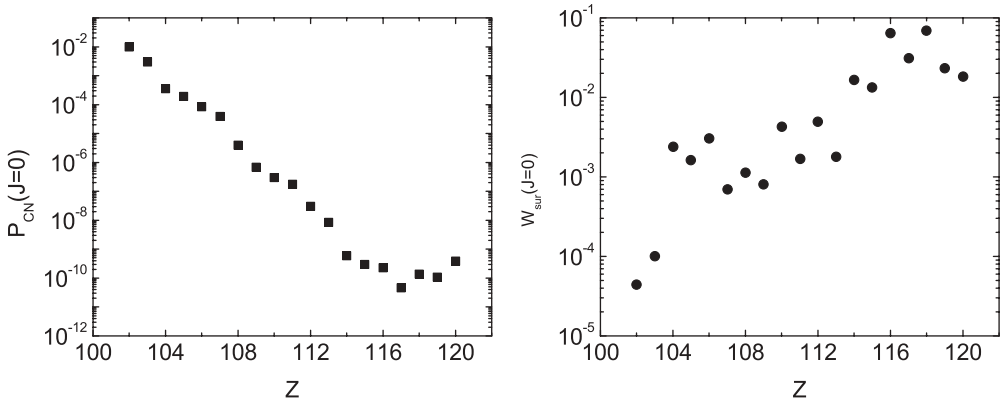

FIG. 6. The fusion and the survival probabilities at $J = 0$ as functions of the charge numbers of the compound nuclei with the same combinations as stated in the caption of Fig. 5.

reaction ^{62}Ni + ^{208}Pb → ^{269}Ds + 1n; however, it is $15\pm^{9}_{6}$ pb for the reaction ^{64}Ni + ^{208}Pb → ^{271}Ds + 1n [1,31]. Further investigations of the isotopic trends are very necessary for predicting the optimal combinations and the optimal excitation energies (incident energies) to synthesize SHN. In Fig. 7 we show the calculated isotopic trends in producing superheavy elements $Z = 110$ and 112 for the reactions ^{A}Ni + ^{208}Pb and ^{A}Zn + ^{208}Pb (squares with lines) and compare them with the results of Adamian *et al.* [32] (diamonds and triangles) and the available experimental data [1] (circles with error bars). We find that the isotopes ^{63,64,65}Ni and ^{67,70}Zn are suitable for synthesizing superheavy elements 110 and 112, respectively. The isotopes ^{64}Ni and ^{67}Zn have larger production cross sections, which is consistent with the results of Adamian *et al.* But for other isotopes, the two methods give slightly different results. For example, our model indicates that ^{70}Zn has a larger cross section for producing element 110 than does the isotope ^{68}Zn. However, the opposite trend is obtained by Adamian *et al.* Therefore, a more accurate description of the three stages of the formation of SHN is needed. Further experimental data are also required to examine the theoretical models. In the DNS model, the isotopic trends are mainly determined by both the fusion and survival probabilities. Of course, the transmission probability of two colliding nuclei can also affect the trends since the initial quadrupole deformations depend on the isotopes. When the neutron number of the projectile is increased, the DNS gets more symmetrical and the fusion probability decreases if the DNS does not consist

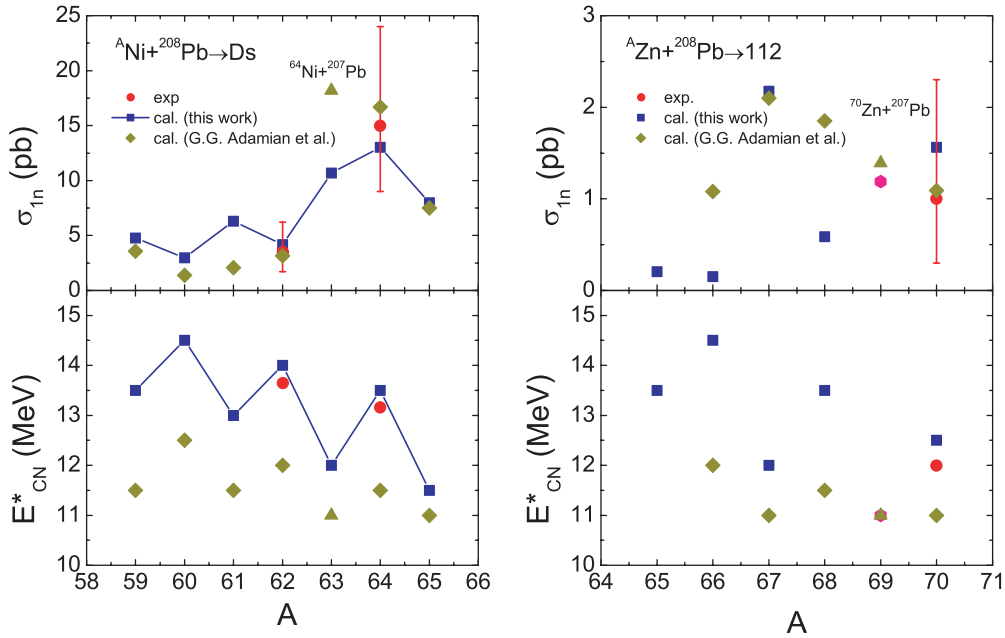

FIG. 7. (Color online) Isotopic dependence of the calculated maximal production cross sections and the corresponding excitation energies in the synthesis of superheavy elements $Z = 110$ and 112 for the reactions ^{A}Ni + ^{208}Pb and ^{A}Zn + ^{208}Pb and compared with the results of Adamian *et al.* [32] and the experimental data [1,4].

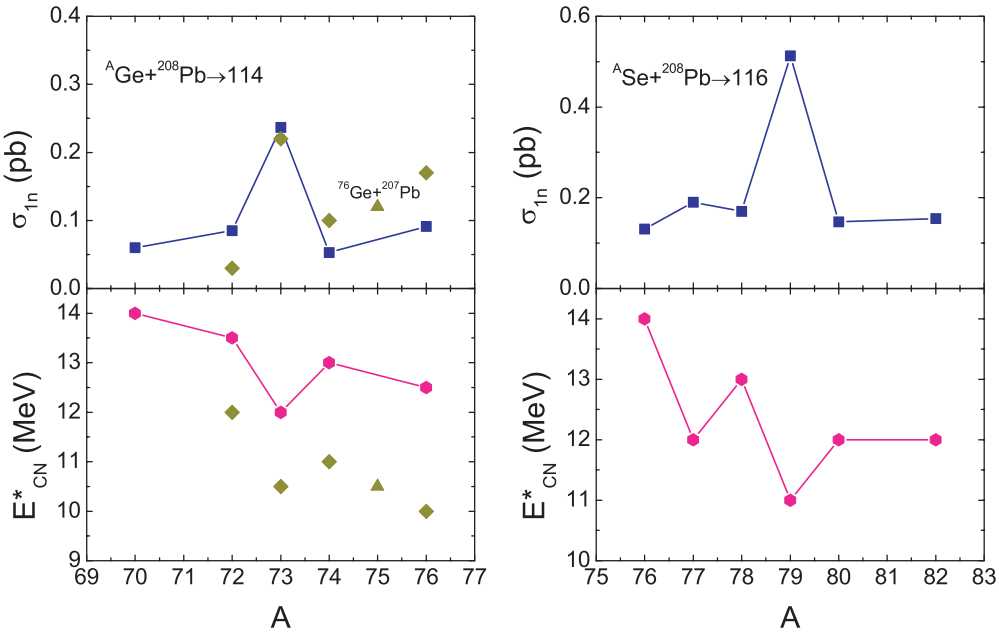

FIG. 8. (Color online) The same as in Fig. 7, but for isotopes Ge and Se to produce superheavy elements $Z = 114$ and 116.

of more stable nuclei owing to a higher inner fusion barrier. A smaller neutron separation energy and a larger shell correction lead to a larger survival probability. The compound nucleus with closed neutron shells has larger shell correction energy and neutron separation energy. With the same procedure, we analyzed the dependence of the production cross sections on the isotopes Ge and Se to produce the superheavy elements $Z = 114$ and 116 shown in Fig. 8 as well as on the isotopes Kr and Sr to synthesize the superheavy elements $Z = 114$ and 116 with a ^{208}Pb target as shown in Fig. 9. The results show that the projectiles ^{73}Ge, ^{79}Se, ^{85}Kr and ^{87,88}Sr are favorable for synthesizing the new superheavy elements $Z = 114$, 116, 118, and 120. The corresponding excitation energies are also given in the figures. The compound nuclei with neutron-rich isotopes ^{76}Ge, ^{80,82}Se, and ^{84,86}Kr are near the subclosure at $N = 172$. These compound nuclei have larger one-neutron separation energies, and the initial combinations' smaller mass asymmetries lead to smaller evaporation residue cross sections.

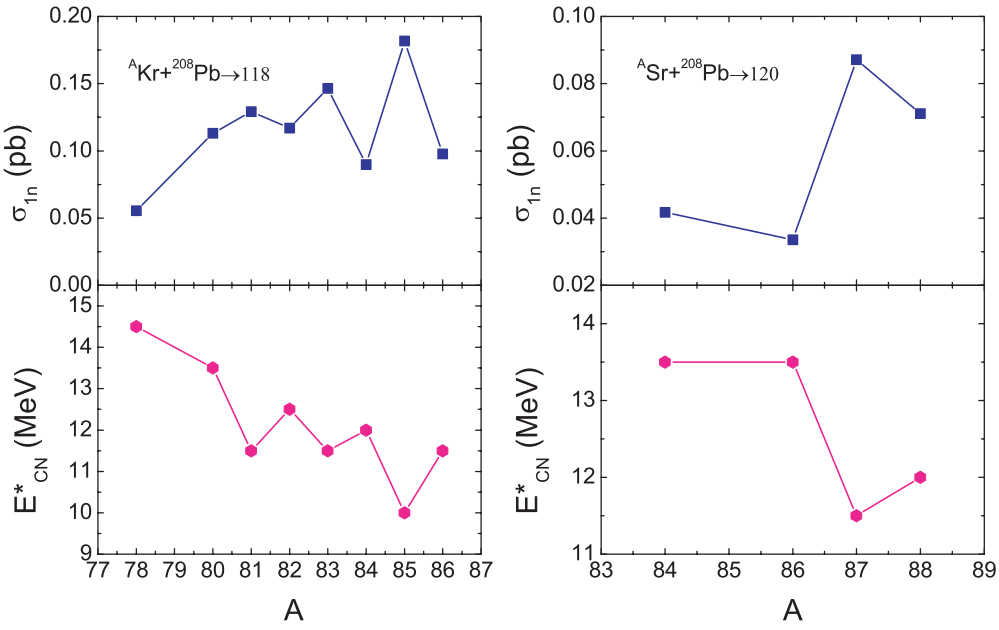

FIG. 9. (Color online) The same as in Fig. 7, but for isotopes Kr and Sr based on ^{208}Pb target.

IV. CONCLUSIONS

Within the DNS concept, a dynamical model is worked out for describing the production of superheavy residues in fusion-evaporation reactions, in which the formation of the superheavy compound nucleus is described by a master equation that is solved numerically and includes the quasifission of the DNS and the fission of the heavy fragments in the nucleon transfer process. By using the DNS model, the fusion dynamics and the evaporation residue excitation functions in cold fusion reactions are investigated systematically. The calculated results are in good agreement with available experimental data within error bars. Isotopic trends in the production of superheavy elements are analyzed systematically. It is shown that the isotopes ^{63,64,65}Ni, ^{67,70}Zn, ^{73}Ge, ^{79}Se, ^{85}Kr, and ^{87,88}Sr are favorable for producing the superheavy elements $Z = 110$, 112, 114, 116, 118, and 120 at the stated excitation energies.

The physical nature of the synthesis of heavy fissile nuclei in massive fusion reactions is very complicated, involving not only certain quantities that crucially influence the whole process but also the dynamics of the process. The coupling of the dynamic deformation and the nucleon transfer in the course of overcoming the multidimensional PES has to be considered in the DNS model. The height of the fission barrier for the heavy or superheavy nuclei, which is mainly determined by the shell correction energies at the ground state and at the saddle point, requires additional study [33]. It plays an very important role in the calculation of the survival probability. Further work is in progress.

ACKNOWLEDGMENTS

One of authors (Z.-Q. Feng) is grateful to Prof. H. Feldmeier, Dr. G. G. Adamian, and Dr. N. V. Antonenko for fruitful discussions and help. This work was supported by the National Natural Science Foundation of China under Grant Nos. 10475100 and 10505016, the Knowledge Innovation Project of the Chinese Academy of Sciences under Grant Nos. KJCX2-SW-N17 and KJCX-SYW-N2, the Major State Basic Research Development Program under Grant No. 2007CB815000, and the Helmholtz-DAAD in Germany.

[1] S. Hofmann and G. Münzenberg, Rev. Mod. Phys. **72**, 733 (2000); S. Hofmann, Rep. Prog. Phys. **61**, 639 (1998).
[2] Yu. Ts. Oganessian, J. Phys. G **34**, R165 (2007); Nucl. Phys. **A787**, 343c (2007).
[3] Yu. Ts. Oganessian, A. S. Iljnov, A. G. Demin *et al*., Nucl. Phys. **A239**, 353 (1975); **A239**, 157 (1975).
[4] G. Münzenberg, J. Phys. G **25**, 717 (1999).
[5] K. Morita, K. Morimoto, D. Kaji *et al*., J. Phys. Soc. Jpn. **73**, 2593 (2004).
[6] Yu. Ts. Oganessian, A. G. Demin, A. S. Iljnov *et al*., Nature (London) **400**, 242 (1999); Yu. Ts. Oganessian, V. K. Utyonkov, Y. V. Lobanov *et al*., Phys. Rev. C **62**, 041604(R) (2000); **69**, 021601(R) (2004); **74**, 044602 (2006).
[7] W. J. Swiatecki, Prog. Part. Nucl. Phys. **4**, 383 (1980).
[8] S. Bjornholm and W. J. Swiatecki, Nucl. Phys. **A391**, 471 (1982).
[9] Y. Aritomo, T. Wada, M. Ohta, and Y. Abe, Phys. Rev. C **59**, 796 (1999).
[10] V. I. Zagrebaev, Phys. Rev. C **64**, 034606 (2001); V. I. Zagrebaev, Y. Aritomo, M. G. Itkis, Y. T. Oganessian, and M. Ohta, *ibid.* **65**, 014607 (2001).
[11] G. G. Adamian, N. V. Antonenko, W. Scheid *et al*., Nucl. Phys. **A627**, 361 (1997); **A633**, 409 (1998).
[12] Z.-Q. Feng, G.-M. Jin, F. Fu, and J.-Q. Li, Nucl. Phys. **A771**, 50 (2006).
[13] P. Reiter, T. L. Khoo, T. Lauritsen *et al*., Phys. Rev. Lett. **84**, 3542 (2000).
[14] W. Li, N. Wang, J. Li *et al*., Eur. Phys. Lett. **64**, 750 (2003); J. Phys. G **32**, 1143 (2006).
[15] A. Diaz-Torres, G. G. Adamian, N. V. Antonenko, and W. Scheid, Phys. Rev. C **64**, 024604 (2001); A. Diaz-Torres, *ibid.* **74**, 064601 (2006).
[16] W. Nörenberg, Z. Phys. A **274**, 241 (1975); S. Ayik, B. Schürmann, and Nörenberg, *ibid*. **277**, 299 (1976).
[17] H. Feldmeier, Rep. Prog. Phys. **50**, 915 (1987).
[18] G. Wolschin and W. Nörenberg, Z. Phys. A **284**, 209 (1978).
[19] J. Q. Li, X. T. Tang, and G. Wolschin, Phys. Lett. **B105**, 107 (1981).
[20] G. G. Adamian, N. V. Antonenko, and W. Scheid, Phys. Rev. C **68**, 034601 (2003).
[21] P. Grangé, J.-Q. Li, and H. A. Weidenmüller, Phys. Rev. C **27**, 2063 (1983).
[22] G. G. Adamian, N. V. Antonenko, S. P. Ivanova, and W. Scheid, Phys. Rev. C **62**, 064303 (2000).
[23] Z.-Q. Feng, G.-M. Jin, F. Fu, and J.-Q. Li, High Energy Phys. Nucl. Phys. **31**, 366 (2007).
[24] G. G. Adamian, N. V. Antonenko, R. V. Jolos *et al*., Int. J. Mod. Phys. E **5**, 191 (1996).
[25] Q. Li, W. Zuo, W. Li *et al*., Eur. Phys. J. A **24**, 223 (2005).
[26] C. Y. Wong, Phys. Rev. Lett. **31**, 766 (1973).
[27] A. Nasirov, A. Fukushima, Y. Toyoshima *et al*., Nucl. Phys. **A759**, 342 (2005).
[28] J.-Q. Li and G. Wolschin, Phys. Rev. C **27**, 590 (1983).
[29] P. Möller *et al*., At. Data Nucl. Data Tables **59**, 185 (1995).
[30] K. E. Gregorich, T. N. Ginter, W. Loveland *et al*., Eur. Phys. J. A **18**, 633 (2003).
[31] S. Hofmann, V. Ninov, F. P. Heßberger *et al*., Z. Phys. A **350**, 277 (1995); **350**, 281 (1995).
[32] G. G. Adamian, N. V. Antonenko, and W. Scheid, Phys. Rev. C **69**, 011601(R) (2004).
[33] R. Smolanczuk, J. Skalski, and A. Sobiczewski, Phys. Rev. C **52**, 1871 (1995).